Dynamics of Poly(propylene sulfide) Studied by Dynamic Mechanical Measurements and Dielectric Spectroscopy

Erwan Nicol, Taco Nicolai,* and Dominique Durand

Chimie et Physique des Matériaux Polymères, UMR CNRS, Université du Maine, 72085 Le Mans Cedex 9, France

Received June 1, 1999; Revised Manuscript Received August 26, 1999

ABSTRACT: Dynamical properties of bulk poly(propylene sulfide) (PPS) were investigated for a range of molar masses between 600 and 50 000 g/mol. The primary and secondary relaxation (α-relaxation and β-relaxation) were studied using dielectric spectroscopy. The local segmental relaxation (α-relaxation) and the chain backbone conformational relaxation were studied using dynamic mechanical measurements. The dynamical properties of PPS are compared to those of poly(propylene oxide) (PPO) and are shown to be very similar. However, the glass transition temperature of PPS decreases strongly for low molar masses, while for PPO it is almost independent of the molar mass down to 400 g/mol.

Introduction

Recently, a novel method was developed to synthesize well-defined monodisperse poly(propylene sulfide) (PPS).[1] Although this polymer was synthesized for the first time in 1961,[2] little is known about its dynamical properties. PPS has the same structure as the better known poly(propylene oxide) (PPO), but with all the oxygen atoms replaced by sulfur atoms. PPO, also known as poly(propylene glycol), is an industrially important polymer, and its dynamical properties have been extensively investigated (see e.g. refs 3−19). A striking feature of PPO is that the glass transition temperature (T_g) depends very weakly on the molar mass (M), even for molar masses down to 400 g/mol. The absence of the effect of free ends on T_g can be attributed to hydrogen bonding which reduces the mobility of the free ends. Earlier measurements of the chain backbone conformational relaxation (Rouse modes) showed an anomalous molar mass dependence which was also attributed to the effect of hydrogen bonding.[4,15] However, more recent work[16] showed that the anomalous molar mass dependence was due to an underestimation of the higher molar masses used in the investigation. Using better defined samples over a wider range of molar mass, it was established that the long time dynamic mechanical and dielectric relaxation can be well described by the Rouse model and that entanglements become important for $M > 4000$ g/mol.

In PPS hydrogen bonding is much weaker than in PPO, and therefore comparison between PPS and PPO will reveal the influence of hydrogen bonding on dynamical properties. In this paper we report a study of the dynamic mechanical and dielectric properties of PPS with a range of molar masses between 600 and 50 000 g/mol. We investigate the local segmental relaxation (α-relaxation) which characterizes the glass transition, the sub-glass relaxation (β-relaxation), and the overall conformational relaxation. Comparison with earlier results on PPO shows that PPS and PPO have very similar properties. Therefore, we can refer to earlier work on PPO for discussion of results that are common and we focus here on the differences between these two polymers.

Experimental Section

Sample Synthesis and Characterization. We have synthesized a series of PPS samples following a procedure detailed in ref 1. Using this procedure, PPS with methylnaphthyl end groups is made. Thiol end-capped PPS was prepared by a different termination step, i.e., an acid−base reaction between the thiolate end groups of the living polymer and the strongly acidic resin Amberlyst15. Details of this procedure will be published elsewhere.

The samples were characterized using size exclusion chromatography (SEC) with on-line light scattering detection. The SEC equipment has been described in detail elsewhere.[20] We have used two sets of columns: Polymer Laboratories MIX-C 5 μm, 600 × 7.5 mm and E-lin 10 μm and MIX-B 10 μm, each 600 × 7.5 mm. The elution liquid is THF using a flow rate of 1 mL/min. The light scattering detection gives access to the molar mass of the larger samples ($M > 10^4$g/mol). The scattered light intensity is too weak for the smaller samples to obtain accurate results. We found that at a given elution volume the molar mass of PPS is 0.74 times the molar mass of polystyrene. To obtain the molar mass distribution for all samples, we used calibration with polystyrene standards assuming that the proportionality between the molar mass of polystyrene and PPS is valid over the whole range investigated. The molar mass distribution of the samples used in this study is shown in Figure 1a. Values of the number-average molar mass (M_n) and the polydispersity index (M_w/M_n) are given in Table 1.

Figure 1a shows that coupling occurred during the synthesis of larger PPS leads to the formation of polymers with twice the molar mass. The fraction of coupled material increases with increasing molar mass. To investigate the influence of the coupling on the experimental results, two samples have been reduced using $LiAlH_4$. In this way the coupled material is split, but some low molar mass material is produced; see Figure 1b.

Dynamic Mechanical Measurements. Dynamic shear measurements were made on a Rheometrics RDA II dynamic spectrometer using parallel-plate geometry at temperatures between 200 and 340 K. The so-called hold mode was used where the gap is corrected for temperature variations of the sample volume. The plate size (diameters 25, 8, and 4 mm) and the imposed deformation (0.1−100%) were adjusted to obtain an accurate torque response while remaining in the linear regime. The shear modulus could be measured in the range $10-10^9$ Pa. We were able to measure very large moduli by using a relatively large sample thickness (2−2.5 mm) in combination with a small plate size. The range of frequencies, f, used was 2×10^{-3}−20 Hz. Temperatures were measured

10.1021/ma990853f CCC: $18.00
Published on Web 10/07/1999

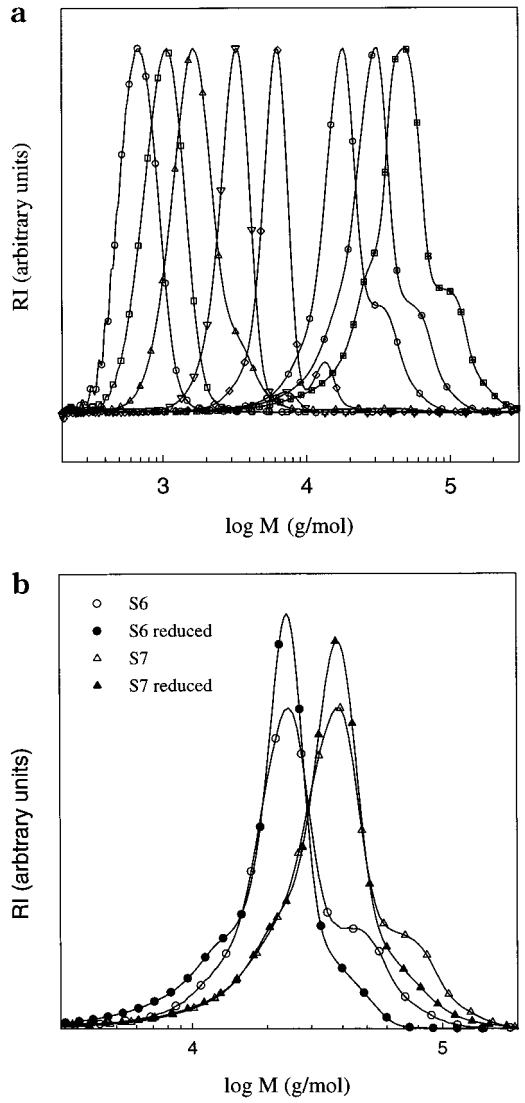

Figure 1. (a) Molar mass distributions of the PPS samples. (b) Effect of reduction of the molar mass distribution of high molar mass PPS samples.

Table 1. Sample Characteristics

	M_n (kg/mol)	M_w/M_n	T_g (K)	T_{gv} (K)	log(τ_0/s)
S1	0.63	1.09	206	203	
S2	0.90	1.11	219	212	−12.7
S3	1.6	1.19	226	221	−12.2
S4	2.9	1.10	231	226	−11.8
S5	6.1	1.14	233	228	−11.3
S6	16.2	1.27	236	230	−10.7
S6[a]	11.9	1.34	236	230	−10.7
S7	23.7	1.37	235	231	−9.7
S7[a]	20.3	1.36	236	231	−9.9
S8	35.8	1.53		231	−9.1

[a] After reduction.

using a thermocouple close to the lower plate. The temperature was stable within ±0.2 K over the whole range used in this study (200−350 K).

Dielectric Spectroscopy. Measurements of the complex dielectric permittivity were made with broad-band dielectric spectroscopy equipment from Novocontrol GmbH. Measurements were made in the frequency range from 10^{-1} up to 10^6 Hz. The samples were kept between two gold-plated stainless steel plates of 20 or 40 mm in diameter with a gap varying between 30 and 500 μm. The sample cell was placed in a cryostat, and the sample temperature was regulated with an accuracy of ±0.1 K and measured with a PT100 sensor in the lower plate of the sample capacitor.

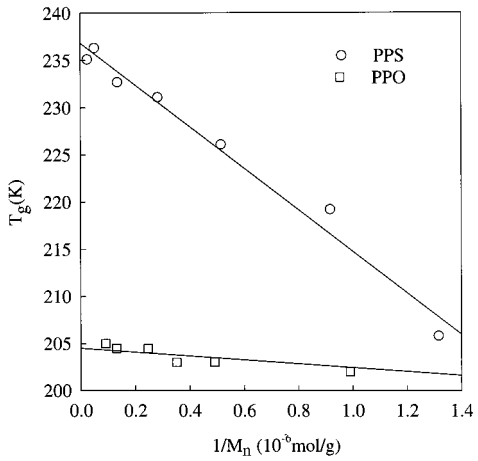

Figure 2. 2. Glass transition temperatures as a function of the inverse number-averaged molar mass. The solid line represents a linear least-squares fit; see eq 1.

Results and Discussion

Glass Transition Temperature. Calorimetric glass transition temperatures were measured using differential scanning calorimetry (DSC). The samples were cooled rapidly to 150 K and then heated at a rate of 10 K/min. Values of T_g taken as the midpoint of the transition are summarized in Table 1 and plotted in Figure 2 as a function of $1/M_n$. The reproducibility is ±2 K. For comparison we also show the results for PPO. A linear least-squares fit gives for PPS

$$T_g = 236 - \frac{2.20 \times 10^5}{M_n}\,(\mathrm{K}) \qquad (1)$$

Contrary to PPO, for PPS the molar mass dependence of T_g is important at small molar masses as observed for other non-hydrogen-bonding polymers.[21] At high molar mass T_g of PPS is 30 K higher than that of PPO.

Dielectric Spectroscopy. Dielectric spectroscopy (DS) shows two relaxation processes. One relatively broad mode (β-relaxation) is observed at temperatures below T_g. The other mode (α-relaxation) is narrower and is observed at temperatures close to and above T_g. In addition, conductivity due to the presence of charged impurities results in an upturn of the loss dielectric permittivity (ϵ'') at frequencies below the α-relaxation. Figure 3a shows the frequency dependence of ϵ'' at different temperatures close to and above T_g for sample S6. The peaks characterize the α-relaxation which merges with the much weaker β-relaxation at high frequencies. The amplitude of the α-relaxation decreases weakly with increasing temperature except at higher temperatures when it merges with the β-relaxation. Figure 3b shows that the data superimpose if ϵ'' is normalized by the maximum value (ϵ''_{max}) and the frequency is normalized by the value of the maximum loss (f_{max}). In the temperature range covered in the experiment the width of the α-relaxation is independent of the temperature. The solid line represents a fit to a generalized exponential (GEX) relaxation time distribution, which was shown to be equivalent to a stretched exponential decay in the time domain: $\epsilon(t) = \epsilon_\infty + \Delta\epsilon \exp[-(t/\tau_0)^\beta]$, with ϵ_∞ the high-frequency value and $\Delta\epsilon$ the relaxation strength. The best fit was obtained with $\beta = 0.47$. Figure 4 shows that the shape of the α-relaxation is independent of the molar mass. The deviation at high frequencies is caused by the β-relaxation. In the

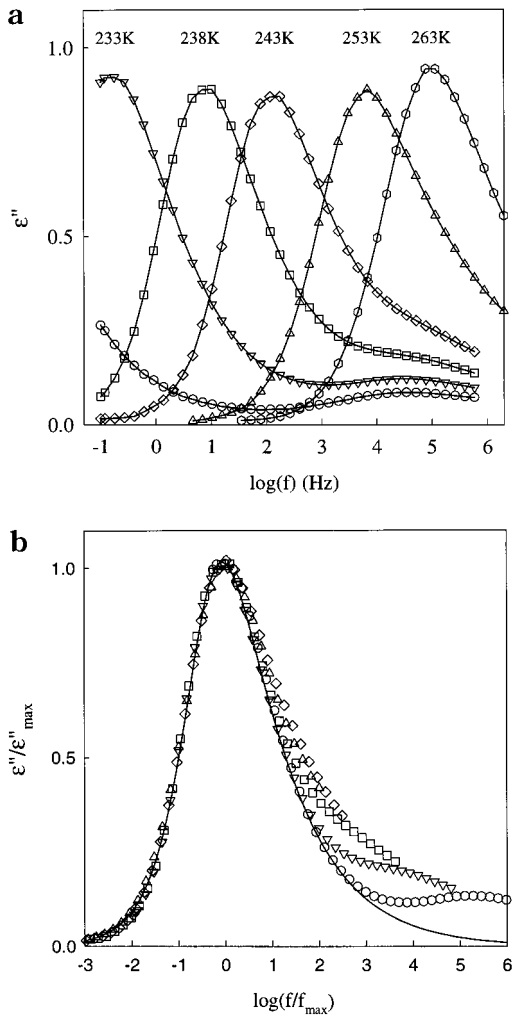

Figure 3. (a) Frequency dependence of the loss dielectric permittivity for sample S6 at different temperatures indicated in the figure. At these temperatures mainly the α-relaxation is observed. (b) Plot of the data shown in (a) after normalization. The solid line represents a fit to the GEX function which corresponds to a stretched exponential decay in the time domain with $\beta = 0.48$.

range investigated the relaxation strength of the α-relaxation is independent of the molar mass: $T\Delta\epsilon \approx 800$.

An Arrhenius representation of the temperature dependence of f_{max} is shown in Figure 5. For clarity, we show only the results of four samples because the results of the high molar mass samples are very close. For PPO we found[16] that the temperature dependence of the characteristic relaxation time defined as $\tau = 1/(2\pi f_{max})$ was the same for different molar masses if plotted as a function of $T - T_{gv}$ where T_{gv} is the temperature at which the maximum loss shear modulus is situated at radial frequency $\omega = 1$ rad/s; see below. T_{gv} is proportional to the glass transition temperature measured by DSC but can be determined with higher accuracy. The values of T_{gv} of the PPS samples are given in Table 1 and are systematically about 5 K smaller than T_g. Figure 6 shows that also for PPS the temperature dependence of τ is independent of the molar mass if plotted as a function of $T - T_{gv}$. The temperature dependence can be well described by the Vogel−Fulcher−Tammann (VFT) equation:

$$\log(\tau) = \log(\tau_0) + \frac{B}{T - T_0} \qquad (2)$$

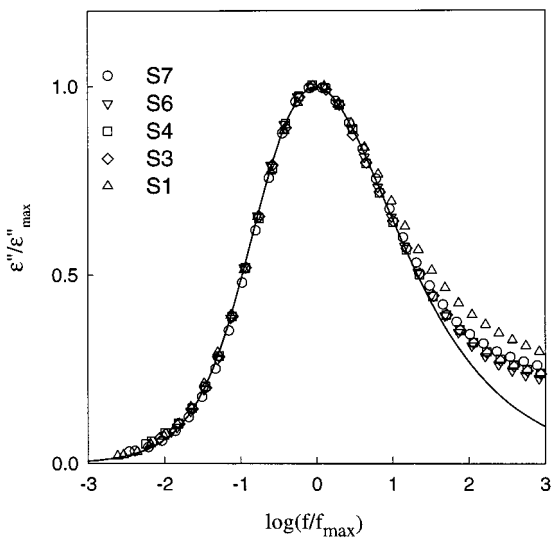

Figure 4. Plot of the normalized frequency dependence of the loss dielectric permittivity for PPS with different molar masses as indicated in the figure. The solid line represents a fit to the GEX function which corresponds to a stretched exponential decay in the time domain with $\beta = 0.48$.

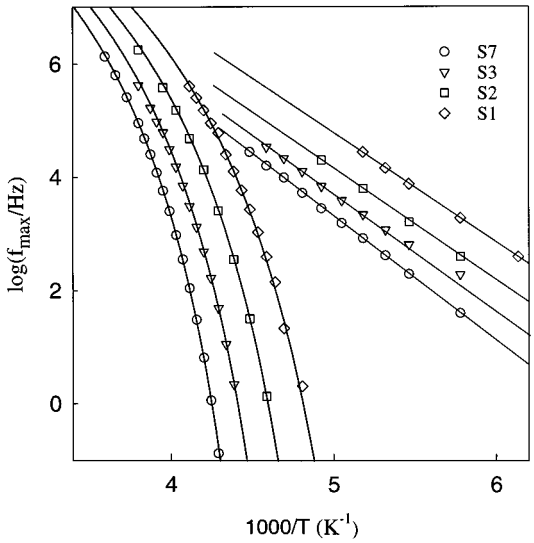

Figure 5. Arrhenius representation of the temperature dependence of the frequency where ϵ'' is maximum for PPS with different molar masses indicated in the figure. Circles indicate the peak position of the α-relaxation while squares indicate the position of β-relaxation. The solid lines through the circles are fits to the VFT equation.

Here $\log(\tau_0)$ is the limiting value at high temperature, B is the apparent activation energy, and T_0 is the "ideal" glass transition temperature. For the α-relaxation of PPS we find $\log(\tau_0/s) = -12.0$, $B = 390$ K, and $T_0 = T_{gv} - 30.0$ K. The shape, the temperature dependence, and the amplitude of the α-relaxation of PPS are close to those of PPO.[16]

Figure 7a shows the frequency dependence of the loss dielectric permittivity (ϵ'') at different temperatures below T_g for sample S6. The peaks characterize the β-relaxation which broadens and decreases in amplitude when the temperature is decreased. The frequency where ϵ'' is maximum has an Arrhenius temperature dependence that is characteristic of sub-glass relaxation; see Figure 5. The activation energy varies little with the molar mass and is 37 ± 1 kJ/mol. Following a method used by Deegan and Nagel[22] to analyze the

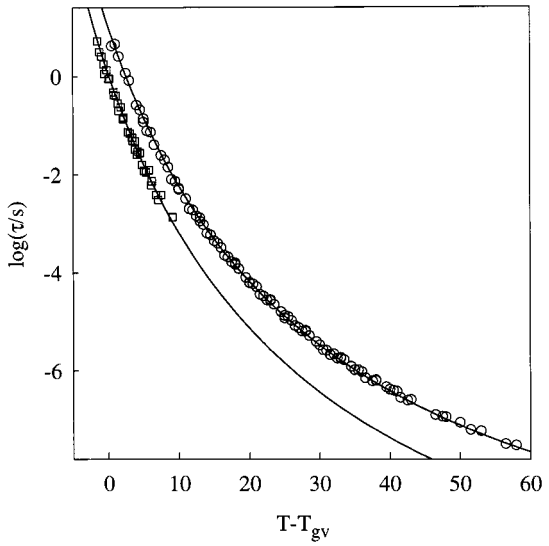

Figure 6. Plot of the characteristic relaxation time $\tau = 1/(2\pi f_{max})$ of the α-relaxation as a function of $T - T_{gv}$ for PPS with different molar masses between 600 and 40 000 g/mol. Circles indicate the results from DS while squares indicate the results from mechanical shear measurements. The solid lines are fits to the VFT equation with the same values for B and T_0, but values of $\log(\tau_0)$ that differ by a factor of 9.

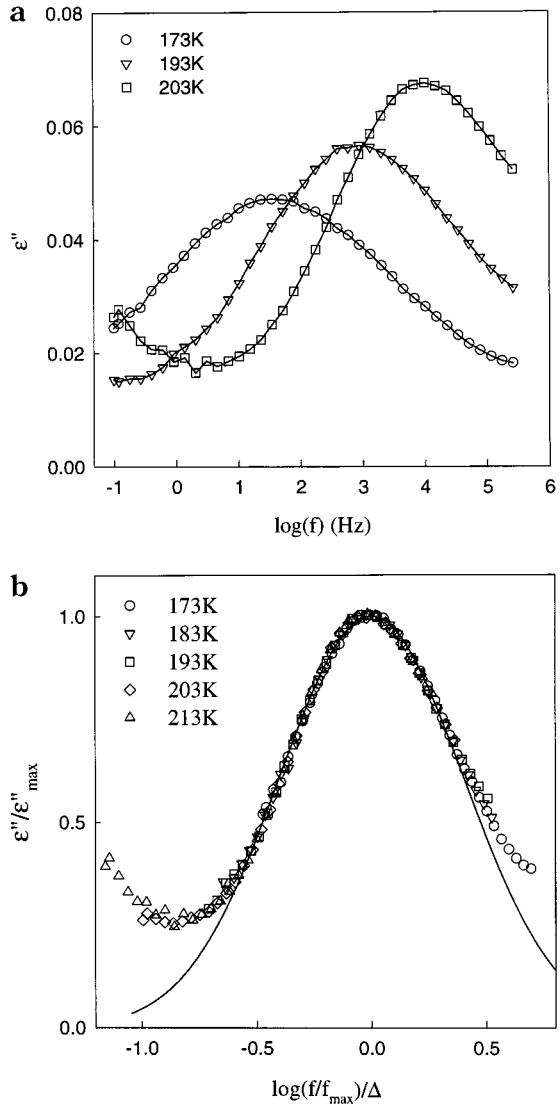

Figure 7. (a) Frequency dependence of the loss dielectric permittivity for sample S6 at different temperatures indicated in the figure. At these temperatures mainly the β-relaxation is observed. (b) Plot of the same data shown in (a) after normalization. The solid line represents a fit to a log-normal relaxation time distribution.

β-relaxation in polybutadiene, we have superimposed the peaks at different temperatures by plotting $\epsilon''/\epsilon_{max}$ as a function of $\log(f/f_{max})/\Delta$, where Δ is the half-width of the peak. The data superimpose to within the experimental error, which shows that the functional form of the β-relaxation is independent of the temperature; see Figure 7b. PPS with other molar masses show a very similar behavior. In fact, representations as in Figure 7b of PPS with other molar masses are the same except for PPS3 and to a lesser extent for PPS5 for which the peak is slightly steeper at the low-frequency side. Δ increases weakly with decreasing temperature from about 4.5 at 213 K to about 5.5 at 173 K and does not depend on the molar mass. The variation of Δ with temperature is similar to that reported by Deegan and Nagel[22] for polybutadiene. The amplitude of the β-relaxation increases linearly with the temperature in the range 173−213 K by about 20%.

Deegan and Nagel[22] suggested that the β-relaxation of polybutadiene is due to a random hopping process over a Gaussian distribution of energy barriers which leads to a log-normal frequency dependence of ϵ''. The solid line in Figures 7b represents a fit to the log-normal distribution. Clearly, the log-normal distribution only describes part of the frequency dependence. At low frequencies there is a transition to the α-relaxation, but the deviation at high frequencies could indicate that the distribution of energy barriers is not Gaussian. For a glass of small molecules Wu[21] found that the β-relaxation was well described by a log-normal distribution even at high frequencies. The width of the β-relaxation was found to increase linearly with $1/T$, but the amplitude was constant. The results on polybutadiene reported by Deegan and Nagel do not cover a sufficiently broad frequency range to establish whether they deviate from a log-normal distribution at high frequencies.

Whatever the origin of the β-relaxation, it is clearly correlated with the α-relaxation. By extrapolating the temperature dependence of the two modes shown in Figure 5 to higher temperatures, we estimate that the two modes merge at about 10^7 Hz and $T - T_{gv} \approx 70$ K. The crossing frequency appears slightly higher for the smallest molar mass, but it is difficult to conclude in view of the rather long extrapolation. In any case it is obvious that end effects influence both the α- and the β-relaxation.

In PPO the β-relaxation is weaker and broader and therefore more difficult to characterize.[16] Nevertheless, we observed that in PPO the width and the amplitude of β-relaxation have a similar weak temperature dependence as observed for PPS. Also for PPO the activation energy is almost independent of the molar mass, and its value is only about 15% smaller than that of PPS. For PPO the two modes merge at about the same frequency and value of $T - T_{gv}$ as for PPS. We noted in ref 16 that for PPO the activation energy is independent of the molar mass even for molar masses down to 400 g/mol for which the contribution of the hydroxyl end group to the dielectric permittivity is important. In addition, the hydroxyl groups contribute to the amplitude of both the α- and the β-relaxation. This makes it unlikely that a specific local motion of the chain backbone is responsible for the β-relaxation.

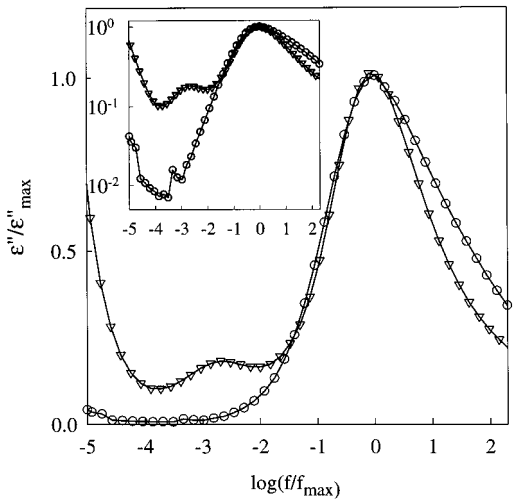

Figure 8. Comparison of the frequency dependence of the loss dielectric permittivity for PPS (circles) and PPO (triangles) with about the same degree of polymerization (70 for PPO and 73 for PPS). The reference temperature is T_{gv} + 23 K. The inset shows the same data in a double-logarithmic representation.

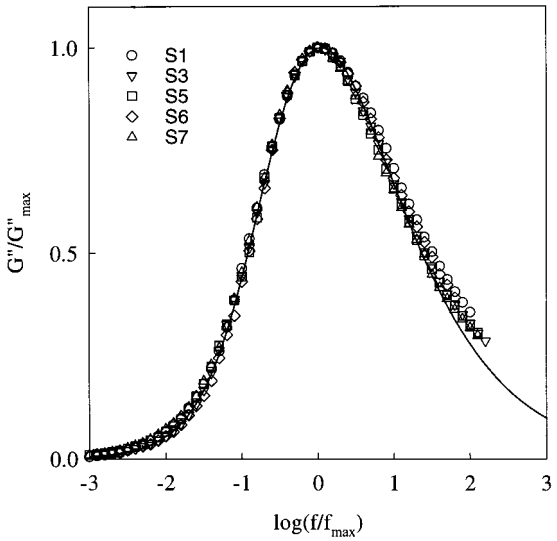

Figure 9. Plot of the normalized frequency dependence of the loss shear modulus for PPS with different molar masses as indicated in the figure. In a semilogarithmic representation only the α-relaxation is visible. The solid line represents a fit to the GEX function which corresponds to a stretched exponential decay in the time domain with $\beta = 0.48$.

In the case of PPO two additional relaxation modes were observed with DS.[16] One mode is situated between the α- and the β-relaxation. It has an Arrhenius temperature dependence and an amplitude that increased strongly after exposure of the sample to a water-rich atmosphere. This mode is most likely induced by the presence of traces of water which are absent in PPS. The second additional mode is slower than the α-relaxation and is molar mass dependent. This mode is due to relaxation of dipoles parallel to the chain backbone and is determined by end-to-end vector fluctuations. In Figure 8 we compare the frequency dependence of ϵ'' for PPO and PPS with about the same degree of polymerization. It seems surprising that simply replacing an oxygen atom by a sulfur atom reduces the strength of the parallel dipole moment to such an extent that it is no longer detectable, while the strength of the total dipole moment is hardly modified. The difference at high frequencies is due to the stronger influence of the merging β-relaxation for PPS.

Shear Modulus. We measured the loss (G'') and storage (G') shear moduli over a wide range of temperatures. Unfortunately, mechanical shear measurements cannot be made over the broad frequency range accessible to DS. In addition, with the setup used in the experiment, it was not possible to measure the β-relaxation. In the frequency range accessible to mechanical measurements the α-relaxation has a strong temperature dependence and can only be measured over a narrow temperature range. In this narrow range the shape of the α-relaxation is independent of the temperature. Figure 9 shows that the shape of the α-relaxation is also independent of the molar mass except perhaps for S1, which appears slightly broader. The solid line represents again a stretched exponential decay in the time domain with $\beta = 0.47$. The value of the maximum loss shear modulus of PPS is within the experimental error independent of the molar mass and the same as for PPO:[15,16] $G''_{max} = 2 \times 10^8$ Pa.

In Figure 6 we have plotted the temperature dependence of $\tau = 1/(2\pi f_m)$ as a function of $T - T_{gv}$. The temperature dependence of τ is independent of the molar mass if plotted as a function of $T - T_{gv}$. τ obtained from G'' is systematically larger than that obtained from ϵ'' by a factor of 9 ± 1. The solid lines in Figure 6 represent nonlinear least-squares fits to eq 1 with the same values of B and T_0 as for ϵ'' (see above) but values of τ_0 that differ by a factor of 9. As mentioned above, the temperature dependence of the α-relaxation in PPS is almost the same as in PPO, and the same systematic difference between the results from DS and mechanical measurements is observed for both polymers. For a discussion of this systematic difference see ref 16.

At lower frequencies the α-relaxation crosses over to the overall conformational relaxation. These two relaxation processes do not have the same temperature dependence. The same effect was observed for PPO and is discussed in detail in refs 15 and 16. It is thus not possible to use time−temperature superposition to obtain a master curve of the whole frequency dependence. However, we can make master curves at a given reference temperature (T_{ref}) by superimposing data at lower temperatures in the high-frequency domain and at higher temperatures in the low-frequency domain. Different samples can be compared if we choose T_{ref} at the same distance from T_{gv}. This procedure leads to the master curves shown in Figure 9. As expected, the conformational relaxation is strongly molar mass dependent. The effect of entanglements is visible for the larger samples but not strong enough to observe a clear plateau in G' or a maximum in G''.

As mentioned in the Experimental Section, high molar mass PPS contains a significant amount of coupled material with twice the molar mass. Figure 11 shows the effect of reduction of PPS on the shear modulus. As expected, only the terminal relaxation is influenced. For these large molar masses DS shows no effect.

The solid lines in Figures 10 and 11 represent nonlinear least-squares fits to a combination of (1) the GEX function (equivalent to a stretched exponential) to describe the α-relaxation, (2) a sum of Rouse normal modes, and (3) a log-normal relaxation time distribution to describe the effect of disentanglement for $M_n > 4000$ g/mol. Earlier we have used this fit procedure success-

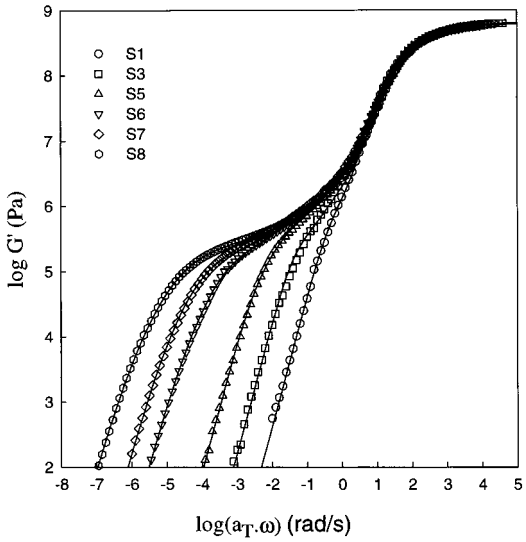

Figure 10. Master curves of the normalized frequency dependence of the storage modulus for PPS with different molar masses as indicated in the figure. The reference temperature is $T_{gv} + 5$ K. The solid lines represent fits to the model discussed in the text.

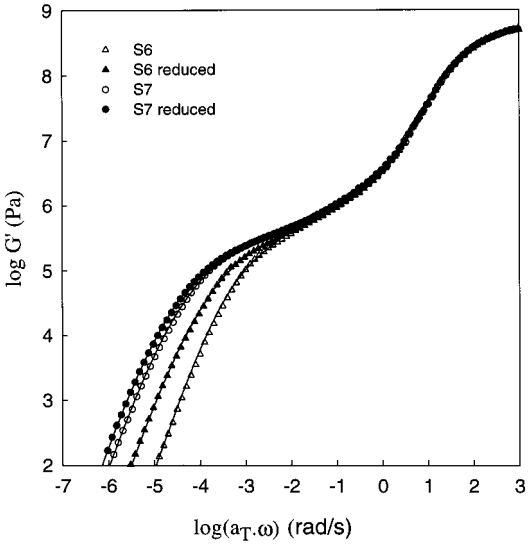

Figure 11. Comparison of the master curves of the storage modulus for S6 and S7 before and after reduction. The reference temperature is $T_{gv} + 5$ K. The solid lines represent fits to the model discussed in the text.

fully for PPO; see for details refs 15 and 16. Figures 10 and 11 show that the model describes the data well also for PPS. Of course, the use of a log-normal distribution to describe the process of disentanglement is arbitrary. But, on one hand, a single-exponential decay is not sufficient to obtain a good fit, and on the other hand, a more complicated distribution is not justified because it is relatively narrow even for the largest molar mass studied here.

We have taken the terminal relaxation time (τ_c) of the conformational relaxation as the slowest Rouse mode for the samples with $M_n < 4000$ g/mol and as the maximum of the log-normal distribution characterizing the disentanglement process for the larger samples. The temperature dependence of τ_c is shown in Figure 12 together with that of the α-relaxation. To show the latter over a wider temperature range, we include the results from DS shifted by a factor of 9. Within the experimental error the temperature dependence of τ_c can be

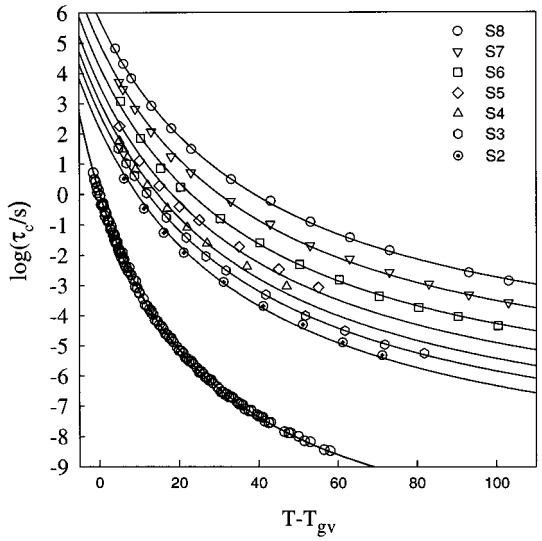

Figure 12. Plot of the terminal relaxation time as a function of $T - T_{gv}$ for PPS with different molar masses between 600 and 50 000 g/mol. For comparison, we also show the characteristic relaxation time of the α-relaxation from mechanical measurements and from DS divided by a factor of 9. The solid lines are fits to the VFT equation.

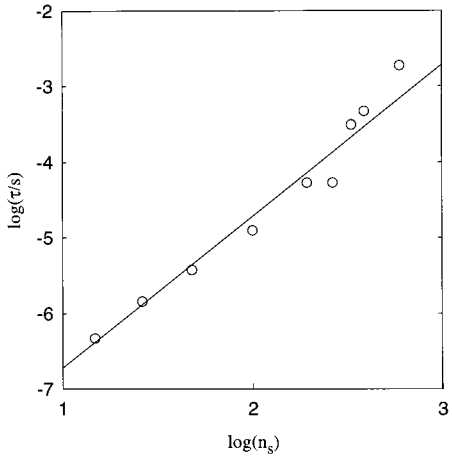

Figure 13. Double-logarithmic representation of the terminal relaxation time as a function of the degree of polymerization. The solid line has slope 2.

described by the VFT equation with the same values for $B = 525$ K and $T_0 = T_{gv} - 43$ K for all molar masses, but different values of $\log(\tau_0)$ shown in Table 1.

In Figure 13 we have plotted the conformational relaxation time at $T = T_{gv} + 100$ K as a function of the number of PPS segments (n_s). The straight line through the data shows that the molar mass dependence is close to that expected for the slowest Rouse normal mode ($\tau_c \propto n_s^2$). At high molar mass the increase is stronger due the influence of entanglements. For many linear polymers $\tau_c \propto n_s^{3.4}$ if the molar mass is much larger than that between entanglements. The transition to this power law dependence is not yet obvious for the range of masses studied here. This is partly due to the choice of the τ_c because the width of the log-normal distribution increases with increasing molar mass. This means that the maximum of the log-normal relaxation time distribution becomes a poorer estimate of the terminal relaxation time. In ref 16 we showed for PPO a plot similar to Figure 13 also at $T = T_{gv} + 100$ K and not at $T = T_{gv} + 130$ K as was erroneously written in the text. Note also that in ref 16 we showed the slowest confor-

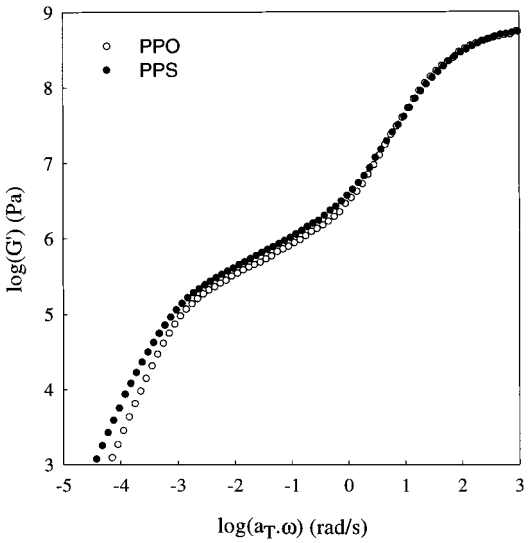

Figure 14. Comparison of the frequency dependence of the storage modulus for PPS and PPO with about the same degree of polymerization (189 for PPO and 193 for PPS). The reference temperature is $T_{gv} + 5$ K.

mational relaxation as observed in DS, which is 2 times smaller than that observed in mechanical shear measurements for reasons explained in ref 16.

The dynamic mechanical properties of PPS are very close to that of PPO with the same number of segments. This is illustrated in Figure 14 where we compare master curves for PPS and PPO with about the same degree of polymerization. The curves almost superimpose which might be expected since the density[24] and the persistence length[25] of both polymers are close. Like for the α-relaxation the temperature dependence of the conformational relaxation in both systems is close. Clearly, hydrogen bonding does not influence the overall conformational relaxation. Earlier it was concluded on the basis of Raman and Brillouin scattering measurements[17,18] that hydrogen bonding stiffens the polymer backbone of PPO. The present results show that even if this stiffening effect exists, it does not have a significant influence on the conformational relaxation.

Summary

DS reveals two relaxation modes for PPS. The temperature dependence of the characteristic relaxation time of the α-relaxation is well described by the Vogel−Fulcher−Tammann equation (eq 2) and is independent of the molar mass after correction for differences in the glass transition temperature. Its shape is independent of the temperature and the molar mass. The characteristic relaxation time of the β-relaxation has an Arrhenius temperature dependence. Its width decreases with increasing temperature while its amplitude increases. Its frequency dependence can be approximated by a log-normal distribution except at high frequencies. The activation energy, width, and amplitude of the β-relaxation do not depend on the molar mass. The two modes merge at a frequency of about 10^7 Hz.

The α-relaxation observed in shear measurements has the same shape and temperature dependence but is systematically slower by a factor of 9. The overall chain backbone relaxation is well described by a series of Rouse normal modes for molar masses up to 4000 g/mol. At higher molar masses relaxation of chain entanglement is observed.

The dynamic properties of PPS as probed by DS and dynamic mechanical measurements are very similar to those of PPO. The most important difference is that the glass transition temperature of PPO is almost independent of the molar mass even at very low molar mass, while PPS shows a decrease of T_g for low molar masses as observed for most polymers.

Acknowledgment. We thank Chantal Bonnans for showing interest in this work and for her help with the synthesis.

References and Notes

(1) Nicol, E.; Bonnans-Plaisance, C.; Levesque, G. *Macromolecules* **1999**, *32*, 4485.
(2) Boileau, S.; Sigwalt, P. *Compt. Rend.* **1961**, *252*, 882.
(3) Schönhals, A.; Schlosser, E. *Phys. Scr.* **1993**, *T49*, 233.
(4) Schlosser, E.; Schönhals, A. *Prog. Colloid Polym. Sci.* **1993**, *91*, 158.
(5) Bauer, M. E.; Stockmayer, W. H. *J. Chem. Phys.* **1965**, *43*, 4319.
(6) Stockmayer, W. H.; Bauer, M. E. *Macromolecules* **1969**, *2*, 647.
(7) Yano, S.; Rabalkar, R. R.; Hunter, S. P.; Wang, C. H.; Boyd, R. H. *J. Polym. Sci., Polym. Phys. Ed.* **1976**, *14*, 1877.
(8) Cochrane, J.; Harrison, G.; Lamb, J.; Phillips, D. W. *Polymer* **1980**, *21*, 837.
(9) Alper, T.; Barlow, A. J.; Gray, R. W. *Polymer* **1976**, *17*, 665.
(10) Wang, C. H.; Fytas, G.; Lilge, D.; Dorfmüller, Th. *Macromolecules* **1981**, *16*, 1363.
(11) Duggal, A. R.; Nelson, K. A. *J. Chem. Phys.* **1991**, *12*, 7677.
(12) Cosgrove, T.; Griffiths, P. C.; Webster, J. R. P. *Polymer* **1994**, *35*, 140.
(13) Fleischer, G.; Helmstedt, M.; Alig, I. *Polymer Commun.* **1990**, *31*, 409.
(14) Johari, G. P. *Polymer* **1986**, *27*, 866.
(15) Randriantoandro, H.; Nicolai, T. *Macromolecules* **1997**, *30*, 2460.
(16) Nicolai, T.; Floudas, G. *Macromolecules* **1998**, *31*, 2578.
(17) Börjesson, L.; Stevens, J. R.; Torell, L. M. *Phys. Scr.* **1987**, *35*, 692.
(18) Yoon, S.; MacKnight, W. J.; Hsu, S. L. *J. Appl. Polym. Sci.* **1997**, *64*, 197.
(19) Sidebottom, D. L.; Bergman, R.; Börjesson, L.; Torell, L. M. *Phys. Rev. Lett.* **1992**, *68*, 3587.
(20) Busnel, J. P.; Degoulet, C.; Nicolai, T.; Woodley, W.; Patin, P. *J. Phys. III* **1995**, *5*, 1501.
(21) Sperling, L. H. *Introduction to Physical Polymer Science;* Wiley and Sons: New York, 1996.
(22) Deegan, R. D.; Nagel, S. R. *Phys. Rev. B* **1995**, *52*, 5653.
(23) Wu, L. *Phys. Rev. B* **1991**, *43*, 9906.
(24) Lal, J.; Trick, G. S. *J. Polym. Sci., Part A-1* **1970**, *8*, 2339.
(25) Nash, D. W.; Pepper, D. C. *Polymer* **1975**, *16*, 105.

MA990853F